



Comparative Evaluation of Green-Synthesized Silver Nanoparticles and Nanoemulsions of *Zygophyllum decumbens* Extracts: Antihyperglycemic and Antimicrobial Activities



Nagwan M. Gabr¹, Soad M. Abd El-Khalik¹, Jaky T. Zaki^{2,1*}, Mahmoud Emam³, Shereen S. El-Mancy⁴, Lina J. M. Abdel-Hafez⁵, and Alaadin E. El-Haddad²

¹Pharmacognosy Department, Faculty of Pharmacy, Helwan University, Cairo 11795, Egypt

²Pharmacognosy Department, Faculty of Pharmacy, October 6 University, Giza 12585, Egypt

³Phytochemistry and Plant Systematics Department, National Research Centre, Dokki, Giza 12622, Egypt

⁴Pharmaceutics and Industrial Pharmacy Department, Faculty of Pharmacy, October 6 University, Giza 12585, Egypt

⁵Microbiology and Immunology Department, Faculty of Pharmacy, October 6 University, Giza 12585, Egypt

Abstract

Disease resistance, including insulin and microbial resistance, is a global challenge. Nano-formulations of plant extracts offer eco-friendly solutions by enhancing biological activities. *Zygophyllum* species, particularly *Zygophyllum decumbens* (*Z. decumbens*), are recognized for their bioactive compounds and potential to manage diabetes and microbial infections. This study developed silver nanoparticles (AgNPs) and nanoemulsion (NE) formulations of *Z. decumbens* ethyl acetate (ET) and *n*-butanol (BT) extracts, assessed their physicochemical properties, and evaluated their antihyperglycemic and antimicrobial activities. AgNPs from both extracts showed enhanced dose-dependent antihyperglycemic activity, where *n*-butanol extract AgNPs (BTN) exhibited significant α -amylase inhibition ($96.09 \pm 0.23\%$ and $99.60 \pm 0.63\%$ at 50 and 500 $\mu\text{g/mL}$, respectively). Both ET and BT AgNPs demonstrated strong antimicrobial effects, particularly against resistant Gram-positive bacteria (MIC 0.3125 and 0.00976 mg/mL, respectively). In contrast, NE formulations showed promising antihyperglycemic activity with limited antimicrobial efficacy. This study highlights the dual biological activity of green-synthesized AgNPs from *Z. decumbens* extracts, surpassing NE formulations in therapeutic potential. AgNPs appear more effective for managing diabetes and combating microbial infections, encouraging further exploration of their mechanisms and clinical applications.

Keywords: *Z. Decumbens*; antihyperglycemic; antimicrobial; nanoformulations; α -amylase; α -glucosidase; pancreatic lipase

1. Introduction

Nanotechnology plays a crucial role in addressing the limitation of drug delivery. Many medications face challenges such as poor bioavailability, limited permeability, and low solubility, which result in suboptimal pharmacokinetics, particularly with certain delivery routes [1]. Several nanopreparations of phytochemicals have recently been successfully developed, demonstrating significant improvements in efficacy [2-4]. Recent studies have demonstrated the potential of various nanoparticles in drug delivery systems, which have been effectively used for drug, vaccine delivery, and controlled release [5]. These nanoparticles have exhibited comparable or even superior activity compared to conventional counterparts [6]. Similarly, our study highlights the role of silver nanoparticles (AgNPs) and nanoemulsions (NE) formulations in improving bioavailability and therapeutic efficacy, further supporting the growing impact of nanotechnology in medicine. The primary goal is to design dosage forms with improved activity. Nanoparticle-based drugs can serve as carriers to deliver therapeutic substances to specific areas of the body or function as therapeutic agents themselves [7]. One notable advantage of formulating plant extracts into pharmaceutical NE is the ease of uniformly incorporating hydrophobic extracts [8] as lipid-based nanocarriers facilitate sustained and controlled release of such hydrophobic extracts, reducing dosing frequency and improving therapeutic outcomes [9]. NE are homogeneous, thermodynamically stable, and isotropic systems composed of an aqueous phase, surfactants/co-surfactants, and an oil phase [10]. Previous studies have highlighted the successful development of NE for phytochemicals [11-13].

Green synthesis of silver and gold nanoparticles (NPs) has become a rapidly growing and significant area within nanotechnology, gaining popularity for its eco-friendly approach and absence of chemical hazards [14]. AgNPs are widely used in medical equipment and as cleaning agents due to their exceptional antimicrobial properties [15, 16]. This non-hazardous method involves synthesizing AgNPs using plant extracts, leveraging their phytoconstituents such as phenolics, flavonoids, and triterpenoids with varying reducing properties. These compounds facilitate the reduction of silver ions (Ag^+) to their metallic form (Ag^0) and act as surface stabilizers, preventing particle aggregation or oxidation [17-19]. Nano-formulations of plant extracts are primarily utilized to treat chronic conditions such as diabetes, cancer, and asthma [20].

*Corresponding author e-mail: jakytalat98@gmail.com; (Jaky T. Zaki).

Received date 27 January 2025; revised date 11 March 2025; accepted date 21 March 2025.

DOI: 10.21608/ejchem.2025.355974.11222

©2025 National Information and Documentation Center (NIDOC)

In diabetes, alpha-amylase and glucosidase enzymes play a key role in glucose metabolism, and inhibiting these enzymes is a critical strategy for managing diabetes by reducing blood glucose levels by preventing polysaccharide breakdown into monosaccharides [21]. Additionally, inhibiting the pancreatic lipase enzyme is particularly significant for managing type II diabetes, especially in obese patients [22].

Plants belonging to the genus *Zygophyllum* are abundant in polyphenols, flavonoids, triterpenes, sterols, and saponins, which contribute to their extensive use in traditional medicine for managing diabetes, fungal infections, hypertension, gout, and rheumatism [23]. However, the bioavailability of these phytoconstituents is typically low due to their inherent characteristics, such as poor permeability, limited aqueous solubility, and reduced absorption of their glycoside forms in the small intestine [24, 25]. Various techniques, including microencapsulation, nano delivery, and microemulsion formulations, have been employed to enhance their bioavailability [26].

There are no reported studies on the nano-formulations or biological activities of *Zygophyllum decumbens* (*Z. decumbens*) aerial parts. Therefore, to address the scarcity of published research, this study was designed to assess and compare the effects of ethyl acetate (ET) and *n*-butanol (BT) extracts of *Z. decumbens* with their respective nano-formulations- green synthesized AgNPs and NE. Characterization of each formulation was conducted using techniques such as ultraviolet (UV)-visible spectroscopy, transmission electron microscopy (TEM), and dynamic light scattering (DLS) for AgNPs, as well as measurements of globule size, polydispersity index (PDI), and zeta potential (ZP) for the NE formulation. These analyses confirmed the successful development of nano-formulations, which were subsequently evaluated for antihyperglycemic activity and antimicrobial efficacy compared to their non-formulated extracts.

2. Results

2.1. Characterization of *Z. decumbens* extracts in AgNPs formulations

Initially, the solutions of both ET and BT extracts exhibited a yellowish color before the addition of AgNO_3 . However, upon adding AgNO_3 , the solutions turned yellowish-brown. **Figure 1** illustrates the UV-visible spectra of AgNPs synthesized by mixing ET or BT extract with 10 mL of 10^{-3} M AgNO_3 solution. The spectra revealed an absorption in the visible range at 345–365 nm for ETN, while BTN displayed absorption at 345–371 nm, attributed to the SPR band [26, 27]. After ten days, no significant shift in the peak position was observed, apart from an increase in absorbance [28, 29].

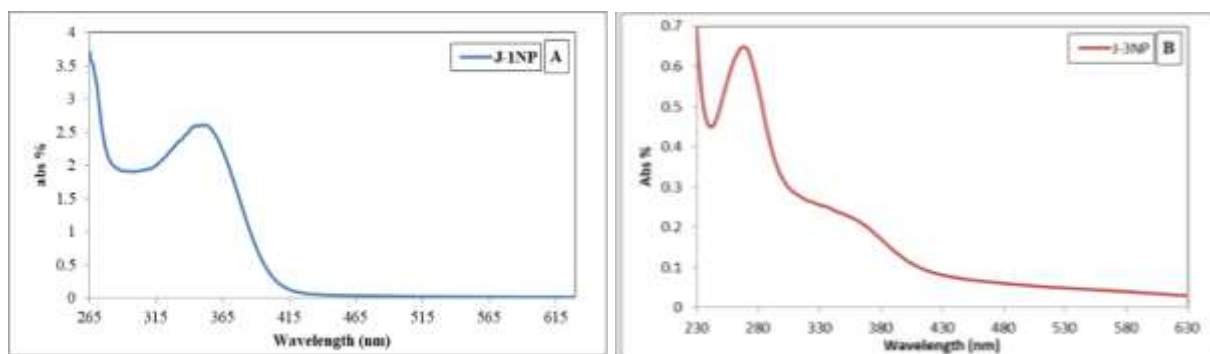


Fig. 1: The surface plasmon resonance band of AgNPs recorded by UV–visible spectra as a function of addition of A; ethyl acetate, and B; *n*-butanol extracts of *Z. decumbens* aerial parts

Figure 2 presents the DLS measurements, including the average PS distribution and ZP. The size distribution of the synthesized AgNPs was analyzed, revealing a mean PS of 77.15 ± 16.64 nm for ETN extract, and 57.57 ± 18.89 nm for the BTN extract (**Figure 2A & 2B**). Additionally, the average ZP values were recorded as -18.7 ± 6.4 mV and -31.3 ± 8.57 mV for ETN and BTN, respectively (**Figure 2C & 2D**). Moreover, TEM analysis reveals that the average PS of the synthesized ETN is 27.13 nm, while that of the BTN is 19.6 nm as shown in **Figure 3 A-F**. The largest particle size (PS) observed was 63.33 nm for ETN and 42.49 nm for BTN

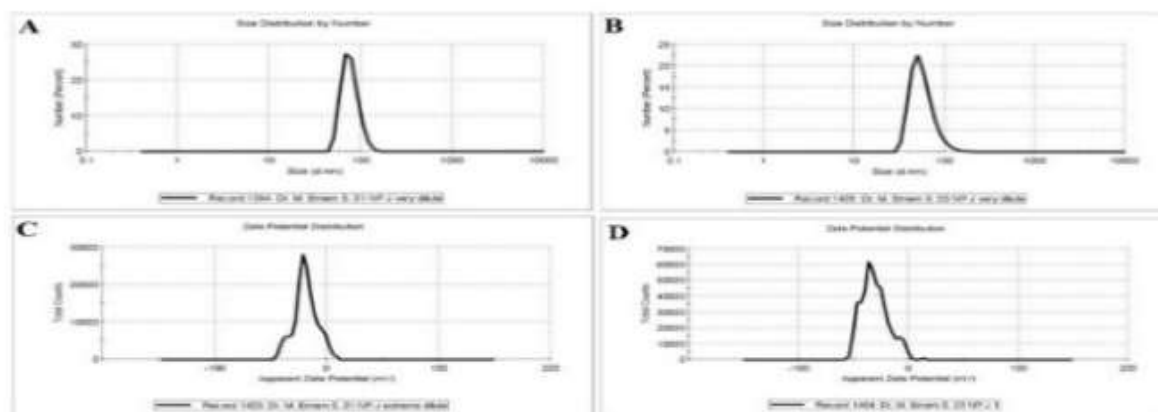


Fig. 2: Particle size distribution of A: ETN and B: BTN extracts and Zeta analysis of C: ETN and D: BTN extracts of *Z. decumbens* aerial parts

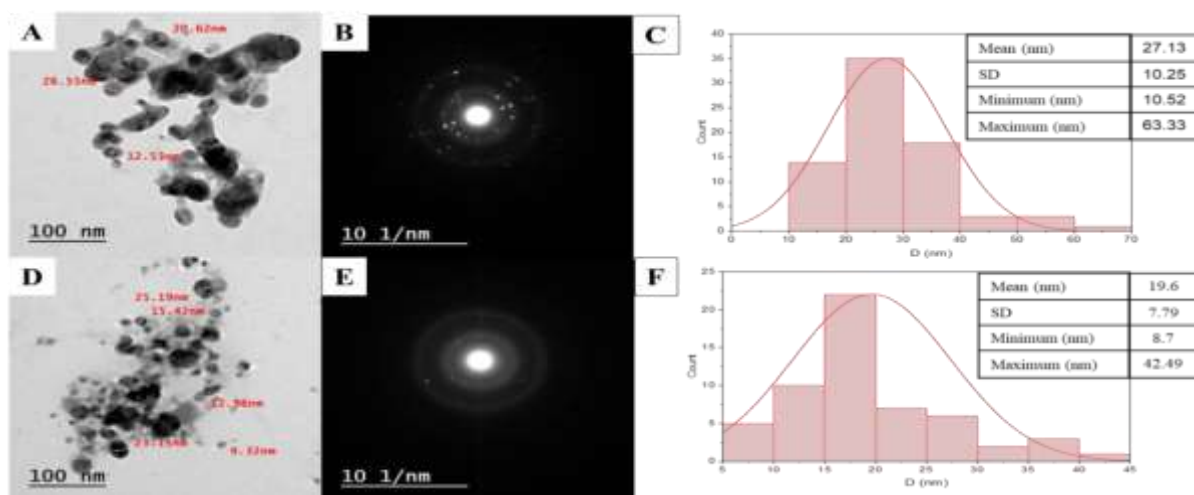


Fig. 3: The TEM images of ETN and BTN extracts of *Z. decumbens* aerial parts; A, D: Low magnification, B, E: Diffraction, and C, F: Particle size distribution, respectively

2.2. Characterization of *Z. decumbens* extracts in NE formulations

The NE systems of both extracts (ETE, BTE) were successfully formulated, exhibiting clear and homogeneous appearances upon visual inspection. Both systems demonstrated small globule sizes within the nanometre range, measuring less than 60 nm (56.2 ± 4.2 and 58.2 ± 0.8 nm for ETE & BTE respectively), along with negative ZP values, as detailed in Table 1.

Table 1: Characterization of nanoemulsions of ethyl acetate and *n*-butanol extracts of *Z. decumbens* aerial parts

| Formula | Visual inspection | Globule size (nm) | Polydispersity index | ZP (mV) |
|---------|-------------------|-------------------|----------------------|-----------------|
| ETE | Clear | 56.2 ± 4.2 | 0.822 ± 0.05 | -13.9 ± 1.7 |
| BTE | Clear | 58.2 ± 0.8 | 0.441 ± 0.06 | -7.1 ± 0.6 |

2.3. Determination of antihyperglycemic activity

Table 2 demonstrates that the ETN extract significantly enhances the percentage inhibition of α -glucosidase and α -amylase (97.25 ± 0.07 , and $97.99 \pm 0.11\%$ at $1000 \mu\text{g/mL}$ and $500 \mu\text{g/mL}$, respectively), when compared to the reference standard drug, acarbose, as well as ET extract. Strong antihyperglycemic activity was observed for the BTN extract, marked by a significant increase in the inhibition percentages of lipase and α -amylase (90.52 ± 3.10 , $99.60 \pm 0.63\%$ respectively) at $500 \mu\text{g/mL}$. For NE, both ETE and BTE extracts exhibited a notable increase in α -glucosidase inhibition percent (86.85 ± 5.62 , $96.22 \pm 2.01\%$ respectively) at $1000 \mu\text{g/mL}$, as well as enhanced lipase inhibitory activities (90.19 ± 6.45 , $95.12 \pm 2.21\%$ respectively) at $500 \mu\text{g/mL}$.

Table 2: Determination of the antihyperglycemic activity of nano-formulated extracts of *Z. decumbens* aerial part

| Samples | % inhibition | | | | | |
|----------|---------------------------------------|-------------------------|------------------------|----------------------|-----------------------------------|----------------------|
| | α -glucosidase inhibitor assay | | Lipase inhibitor assay | | α -amylase inhibitor assay | |
| | $100 \mu\text{g/mL}$ | $1000 \mu\text{g/mL}$ | $50 \mu\text{g/mL}$ | $500 \mu\text{g/mL}$ | $50 \mu\text{g/mL}$ | $500 \mu\text{g/mL}$ |
| ET | 46.79 ± 2.46 | 63.89 ± 3.28 | 61.18 ± 6.78 | $87.73 \pm 6.19^*$ | 19.67 ± 0.29 | 49.71 ± 3.89 |
| ETN | 67.13 ± 3.67 | 97.25 ± 0.07 | N/A | 87.46 ± 3.29 | N/A | 97.99 ± 0.11 |
| ETE | 38.66 ± 3.12 | 86.85 ± 5.62 | 60.46 ± 3.31 | 90.19 ± 6.45 | 20.07 ± 0.47 | 39.34 ± 2.52 |
| BT | 95.65 ± 1.36 | 99.82 ± 1.85 | 45.62 ± 5.12 | 64.38 ± 2.89 | N/A | N/A |
| BTN | 95.53 ± 0.39 | 97.24 ± 0.05 | 58.00 ± 4.36 | 90.52 ± 3.10 | 96.09 ± 0.23 | 99.60 ± 0.63 |
| BTE | 90.07 ± 0.70 | 96.22 ± 2.01 | 85.79 ± 5.14 | 95.12 ± 2.21 | N/A | N/A |
| Standard | Acarbose | | Orlistat | | Acarbose | |
| | $10.08 \mu\text{g/mL}$ | $161.25 \mu\text{g/mL}$ | $0.001 \mu\text{g/mL}$ | $0.1 \mu\text{g/mL}$ | $7.8 \mu\text{g/mL}$ | $125 \mu\text{g/mL}$ |
| | 9.26 ± 0.42 | 84.54 ± 1.54 | 33.70 ± 1.22 | 73.30 ± 6.13 | 38.47 ± 3.43 | 91.68 ± 1.08 |

*ET extract was tested at $250 \mu\text{g/mL}$ as it represents 100% inhibition, *N/A indicates no activity, *ET: Ethyl acetate extract, *BT: *n*-Butanol extract, *ETN: Ethyl acetate extract silver nanoparticle, *BTN: *n*-Butanol extract silver nanoparticle, *ETE: Ethyl acetate extract nanoemulsion, *BTE: *n*-Butanol extract nanoemulsion

2.4. Determination of antimicrobial activity

The results in Table 3 reveal that among the four nano-formulations tested, only ETN and BTN extracts exhibited significant antimicrobial activity against the selected Gram-negative and Gram-positive bacterial species, with a notable reduction in MIC compared to both their original corresponding extract and the reference standard ciprofloxacin. Additionally, these extracts demonstrated strong antifungal activity against the *C. albicans* strain, outperforming fluconazole.

Table 3: Determination of Antimicrobial activity of nano-formulated extracts of *Z. decumbens* aerial parts

| <i>M.os</i> | ET | | ETN | | BT | | BTN | | Fluconazole | | Ciprofloxacin | |
|----------------------|---------|--------------|---------|--------------|---------|--------------|---------|--------------|-------------|--------------|---------------|--------------|
| | IZ (mm) | MIC (mg/m L) | IZ (mm) | MIC (mg/m L) | IZ (mm) | MIC (mg/m L) | IZ (mm) | MIC (mg/m L) | IZ (mm) | MIC (mg/m L) | IZ (mm) | MIC (mg/m L) |
| <i>E. coli</i> | 19±0.60 | 0.625 | 22±0.54 | 0.078 | 19±0.55 | 0.312 | 30±0.15 | 0.00976 | N/A | N/A | 29±0.35 | 0.00976 |
| <i>P. aeruginosa</i> | 30±0.56 | 0.625 | 33±0.5 | 0.156 | 28±0.45 | 0.625 | 32±0.35 | 0.039 | N/A | N/A | 32±0.25 | 0.00976 |
| <i>S. aureus</i> | N/A | N/A | 19±0.25 | 0.3125 | 20±0.60 | 1.25 | 35±0.8 | 0.00976 | N/A | N/A | 30±0.27 | 0.00976 |
| <i>C. albicans</i> | 25±0.57 | 0.156 | 27±0.4 | 0.039 | 28±0.5 | 0.625 | 33±0.2 | 0.00976 | 20±0.40 | 0.747 | N/A | N/A |

* MIC of ETE, BTE was >5 mg/mL & inhibition zone diameter varied between 10-12mm against all microorganisms, *N/A indicates no activity,

*ET: Ethyl acetate extract, BT: n-Butanol extract, ETN: Ethyl acetate extract silver nanoparticle, BTN: n-Butanol extract silver nanoparticle,

ETE: Ethyl acetate extract nanoemulsion, BTE: n-Butanol extract nanoemulsion

3. Discussion

Nanotechnology is a multidisciplinary field that enables the manipulation of matter at the atomic and molecular levels to create innovative applications. Among its wide range of products and uses, nanomaterials hold significant clinical potential in medicine due to their nanoscale properties [30]. The development of drugs in nano-formulations has revolutionized modern medicine by enhancing therapeutic agents' efficacy, safety, and bioavailability. Nanotechnology enables the delivery of drugs at the molecular level, allowing for targeted therapy that minimizes side effects and improves therapeutic outcomes. Nano-formulations enhance drug solubility, stability, and bioavailability, ensuring sustained and controlled release [6, 7]. In nano-formulations characterization, the change in color of the crude extracts is due to the property of quantum confinement, which is a size-dependent property of NPs that affects their optical properties. For both ETN and BTN, the increasing intensity of the SPR band suggested that more Ag⁺ ions were converted to AgNPs. Also, the steady absorbance peak indicated that the colloidal AgNPs solution of both extracts remained stable over an extended period and that additional particles did not assemble. Diabetes mellitus is one of the most common endocrine disorders, which arises due to insufficient insulin production. Diabetes mellitus is characterized by symptoms such as hyperglycaemia, polyphagia, polydipsia, and weight loss. Natural products, with insulin-potentiating factors, play a crucial role in improving glucose metabolism. Utilizing these products offers a practical and cost-effective approach to managing diabetes, particularly in developing countries. Plants of the genus *Zygophyllum* are known to be rich in phenolic compounds, flavonoids, and triterpenoidal saponins [23, 25], which have been reported to regulate starch digestion and reduce blood glucose levels [25, 31]. AgNPs have also shown significant inhibitory effects on carbohydrate-metabolizing enzymes [32]. The significant increase in the percentage inhibition of α -glucosidase and α -amylase by ETN at 1000 and 500 μ g/mL compared to that of the ET can be justified by the synergistic effects of nanoparticle synthesis. Green synthesis with ET enhances the bioactivity of its phytoconstituents via nanoscale AgNPs properties. These NPs provided increased surface area thus facilitating greater interaction with enzyme targets, and improved the solubility, stability, and bioavailability of the bioactive compounds, leading to more effective enzyme inhibition compared to the non-formulated ET and allowing better penetration and interaction with enzyme active sites due to their nanoscale size.

Triterpenoid saponins, in particular, are bioactive compounds capable of inhibiting pancreatic lipase, the enzyme responsible for fat breakdown into absorbable molecules [33]. This property likely underpins the significant inhibition achieved with BT and BTN. BTN significantly outperformed BT showing a marked increase in lipase inhibition percentage (90.52±3.10% at 500 μ g/mL) compared to the BT (64.38±2.89% at the same dose). This is likely due to the green synthesized NPs improved bioavailability and surface area. BTN exhibited significantly enhanced α -amylase inhibition percent (96.09±0.23% at 50 μ g/mL and 99.60±0.63% at 500 μ g/mL) compared to the absence of data for the BT suggesting that the nanoparticle synthesis activates or stabilizes bioactive compounds responsible for α -amylase inhibition. It is worth mentioning that both ETN and BTN exhibit superior inhibition percentages for α -glucosidase and α -amylase compared to acarbose, particularly at higher doses, which highlights the potential of the NPs as a more effective alternative for carbohydrate-digesting enzyme inhibition.

The significant improvement of α -glucosidase inhibition percent caused by ETE at 1000 μ g/mL (86.85%) over that of ET is likely due to enhanced dispersion and solubility of bioactive compounds in the NE system. Although BT showed exceptionally high inhibition (95.65% at 100 μ g/mL, 99.82% at 1000 μ g/mL) indicates that it is rich in highly potent α -glucosidase inhibitors, its corresponding BTE slightly reduced α -glucosidase inhibition (90.07% at 100 μ g/mL, 96.22% at 1000 μ g/mL) suggesting some loss of synergistic effects due to encapsulation as well as possible potential interference from the nanoemulsion's stabilizers or surfactants [10, 34].

The dramatic increase in lipase inhibition by BTE (85.79% at 50 μ g/mL, 95.12% at 500 μ g/mL) is likely due to enhanced solubility and dispersion of bioactive compounds in the NE, in addition to improved enzyme interaction facilitated by the smaller droplet size and better stability of the NE system [34, 35].

Regarding the assessment of antimicrobial activity, AgNPs show significantly lower MIC values compared to their respective non-formulated extracts. BTN even displayed promising activity across all microorganisms, with MIC values comparable to or better than the standard drugs (ciprofloxacin and fluconazole). This highlights the role of NPs in improving antimicrobial activity by increasing bioavailability and targeting efficiency. The nanoscale size of AgNPs alters the physical characteristics of the extracts, offering a larger surface-to-volume ratio. This enhances the interaction with bacterial and fungal

cell walls, increasing their permeability. These interactions disrupt the respiratory chain and interfere with cell division, ultimately leading to cell death [36]. Both Gram-positive (*S. aureus*) and fungal strain (*C. albicans*) showed higher susceptibility to ETN and BTN than Gram-negative bacteria (*E. coli* and *P. aeruginosa*) which can be attributed to structural differences in the microbial cell membranes that influence nanoparticle penetration and activity [36].

Unfortunately, the NE formulations displayed only mild antimicrobial activity. This may be attributed to the extract's encapsulation within the lipid phase, which could limit its immediate availability to interact with microbial cells. Additionally, surfactants in NE might interfere with the antimicrobial effects or create barriers that restrict their interaction with microbial targets [11, 37].

4. Experimental

4.1. Chemicals and Reagents

The enzymes used were porcine pancreatic α -amylase, α -glucosidase from *Saccharomyces cerevisiae* ATCC 204508 (*S. cerevisiae*), and pancreatic lipase from the pig pancreas (CAT numbers: A3176, G5003, & L3126 respectively). The substrates utilized included para-nitrophenyl β -D-glucopyranoside (pNPG), 2-chloro-4-nitrophenyl- α -D-maltotriose, and para-4-nitrophenyl dodecanoate (pNPD) (CAT numbers: N7006, 93834, & 61716 respectively), along with isopropyl myristate (IPM) and Tween 80, all of which were acquired from Sigma-Aldrich, USA. Polyethylene glycol 400 (PEG400) was purchased from Fluka, Buchs, Switzerland. Other chemicals and standards were of analytical grade.

4.2. Plant Material and Extraction

In April 2022, *Z. decumbens* was gathered from Wadi Hagol on the Cairo-Suez Road, Cairo, Egypt with authorization from the Agricultural Research Centre, Cairo, Egypt. The plant was collected under the guidance and identification of a specialized taxonomist at the Horticultural Research Institute (HRI), Flora and Phyto-taxonomy Research Department, Agricultural Research Centre, Giza, Egypt. The collected specimen was verified against herbarium sheets stored at HRI and was assigned voucher number 4752 (CAIM).

At room temperature (rt), 1 Kg of shade-dried aerial parts of *Z. decumbens* was extracted using a cold maceration method with 70% ethanol (2L \times 7). The extract was filtered through Whatman No. 1 filter paper, and the solvent was concentrated using a rotary evaporator (Buchi, AG, Switzerland). The concentrated extract (70g) was suspended in 300 mL of distilled water and defatted with petroleum ether (500mL \times 6). The defatted extract was then fractionated sequentially with ethyl acetate and *n*-butanol (500mL \times 3 each) and dried under vacuum yielding dried residues (1.7g and 2g of ET and BT respectively).

4.3. Preparation of AgNPs

AgNPs were synthesized at rt by mixing 10 mL of AgNO₃ solution (1 mM) with 30 μ L of ET and BT extracts from a stock solution (0.030 g extract dissolved in 2.5 mL solvent that derived from), forming ETN and BTN nanoparticles, respectively. The mixture was shaken thoroughly and allowed to stand in the dark. Purification of the AgNPs involved two cycles of centrifugation at 10,000 rpm for 10 minutes, followed by re-dispersion in deionized water to remove impurities. Additionally, the influence of extract concentration on the size and yield of the biosynthesized NPs was investigated [38].

4.4. Characterization of AgNPs

The band metal wavelength (nm) was detected using a V-730 UV-visible spectrophotometer (JASCO, Japan). The Nicomp™ 380 ZLS size analyzer (USA) evaluated the average size, size distribution, and ZP by DLS. Laser light scattering at 170° was used to detect particle size (PS), with ZP measured at 18°. Furthermore, the PS and form of the produced NPs were studied using TEM (HR-TEM, JEM-2100 PLUS, Jeol, Japan) operating at 200 KV [39].

4.5. Preparation and characterization of NE

NE systems were formulated for both ET and BT extracts. The NE composition included 10% IPM as the oil phase, 40% Tween 80, 20% PEG400, 20% ethanol as the surfactant-cosurfactant mixture, and 10% water as the aqueous phase. The process began by mixing the extracts with IPM using a magnetic stirrer (IKA, MAG HS7, Germany). The surfactant-cosurfactant mixture was added and stirred until the extracts were fully dissolved. Finally, water was incorporated, and the mixture was stirred for 15 minutes to achieve a homogeneous ethyl acetate nanoemulsion (ETE) and butanol nanoemulsion (BTE). Each NE was evaluated through visual inspection and characterized by measuring globule size, PDI, and ZP using a Zeta sizer (ZS, Malvern, UK) at a temperature of 25 \pm 2°C. Each NE was diluted 100-fold with double-distilled water for analysis, and measurements were conducted in triplicate [40].

4.6. Determination of Biological Activity

4.6.1. Determination of Antihyperglycemic Activity

Assessment of the antihyperglycemic activity of the extracts (ET, BT) and their corresponding nano-formulations (ETN, ETE, BTN, and BTE) was conducted using three distinct parameters:

4.6.1.1. α -Glucosidase Inhibition Assay

The assay was conducted using α -glucosidase (50 μ L, 0.6 U/mL) in a phosphate buffer (0.1 M, pH 7). Samples (25 μ L) and a blank were incubated at 37 °C for 10 minutes. Following, 25 μ L of pNPG (3 mM) in phosphate buffer (pH 7) was added as the substrate, and the mixture was incubated for an additional 5 minutes at 37 °C. A stock solution of acarbose (2 mM) was prepared in phosphate buffer (100 mM, pH 7), with subsequent dilutions in water (15.625 and 250 μ g/mL) to achieve final concentrations of 100 and 1000 μ g/mL in methanol. The assay was performed in a 96-well microplate (08-772-2C, Fisher Scientific, USA), and **glucosidase** activity was determined by measuring the release of p-nitrophenol at 405 nm using a FluoStar Omega microplate reader (USA) [41].

4.6.1.2. Pancreatic Lipase Inhibition Assay

Lipase activity was assessed by measuring the conversion of para-nitrophenyl palmitate to p-nitrophenol using a FluoStar Omega Microplate Absorbance Reader (USA). Orlistat, a reference standard, was tested at 10 and 100 nM. Samples were

dissolved in dimethyl sulfoxide and then diluted in methanol to achieve 50 and 500 $\mu\text{g/mL}$ final concentrations. The assay was performed in a 96-well microplate. Each well contained 140 μl of Tris buffer (pH 8) mixed with 20 μl of the sample or blank. Subsequently, 20 μl of porcine lipase solution (2 mg/mL in Tris buffer) was added, and the mixture was incubated at 37°C for 10 minutes. The reaction was initiated by adding 20 μl of pNPD solution (10 mM in isopropanol) and incubating at 37°C for an additional 30 minutes. Lipase activity was determined by measuring the release of *p*-nitrophenol at 405 nm using the microplate reader [41].

4.6.1.3. α -Amylase Inhibition Assay

Samples were tested at final concentrations of 50 and 500 $\mu\text{g/mL}$ in methanol, while acarbose stock solutions were prepared at concentrations of 0.1 and 1 $\mu\text{g/mL}$. The assay was conducted using a 96-well microplate. Each well contained 140 μl of phosphate buffer (50 mM, 0.9% NaCl, pH 7) mixed with 20 μl of either the sample or blank. Next, 20 μl of amylase enzyme solution (1 mg/mL in phosphate buffer, pH 7) was added, and the mixture was incubated at 37°C for 15 minutes. Subsequently, 20 μl of the substrate solution (0.375 mM in phosphate buffer) was added, followed by an additional 10-minute incubation at 37°C. Enzyme activity was evaluated by measuring the release of *p*-nitroaniline at 405 nm using a FluoStar Omega microplate reader (USA) [42]. The following formula was applied to calculate the inhibition percentage of α -glucosidase, pancreatic lipase, and α -amylase

$$\% \text{Inhibition} = \left(\frac{\text{Abs. blank} - \text{Abs. sample}}{\text{Abs. blank}} \right) \times 100$$

Abs. blank: is the absorbance of the control (blank, without inhibitor); Abs. sample: is the absorbance with the inhibitor present.

4.62. Antimicrobial Activity

4.6.2.1. Materials

Microbial isolates were obtained from the microbiology lab, Faculty of Pharmacy, Cairo University. Gram-positive bacteria (*Staphylococcus aureus* ATCC 25923) were cultured on Mueller Hinton agar (MHA) (Difco™, Strasbourg, France) for 24 hours at 37°C. In contrast, Gram-negative bacteria (*Pseudomonas aeruginosa* ATCC 9027 and *Escherichia coli* ATCC 8739) were grown on Tryptic Soya Agar (TSA) (Difco™, Strasbourg, France) for 24 hours at 37°C. Fungal isolate (*Candida albicans* ATCC 10231) were cultured on Sabouraud Dextrose Agar (SDA) (Hi Media Laboratories, USA) for 48 hours at 25°C.

4.6.2.2. Broth micro-dilution method

A single colony from each isolate was subsequently inoculated into 2 mL of its respective medium and incubated overnight. The broth microdilution method was employed for assessing antimicrobial susceptibility. Using a 96-well microtitration plate, two-fold serial dilutions of the samples were prepared in Mueller Hinton broth at concentrations ranging from 2.5 to 0.078 mg/mL. A microbial inoculum, prepared from a standardized suspension adjusted to 0.5 McFarland scale, was added to each well. The inoculated plates were then incubated under optimal conditions for each microorganism. The minimum inhibitory concentration (MIC) defined as the lowest concentration of the tested plant extract that completely inhibited microbial growth in the wells was recorded [27].

4.6.2.3. Cup agar diffusion method

All microbial cultures were standardized to an optical density (OD) of 0.5 at 600 nm. MHA, TSA, and SDA plates were inoculated with 100 μl of the corresponding microbial isolates. Subsequently, 5 mm wells were filled with 100 μl of the sample, prepared in sterile water at a 5 mg/mL concentration. The plates were then incubated at 37°C for 24 hours for bacterial isolates and at 25°C for 48 hours for fungal isolate. The inhibition zones (IZ) were measured in millimeters, and the standard deviation was calculated based on the mean inhibition zone values obtained from three independent repetitions of the experiment.

5. Conclusion

The study highlights the potent antimicrobial and antihyperglycemic activities of *Zygophyllum decumbens* extracts and their nanoformulations. Formulating the extracts into silver nanoparticles (AgNPs) significantly enhanced biological efficacy, particularly antimicrobial activity. Ethyl acetate AgNPs exhibited the strongest inhibition against *E. coli* and *P. aeruginosa*. Moreover, the *n*-butanol AgNPs demonstrated superior antimicrobial effects against *S. aureus* and *C. albicans*. Regarding the antidiabetic activity, nano-formulations significantly enhanced enzymatic inhibition. *n*-butanol AgNPs displayed the highest α -glucosidase inhibition and lipase inhibition, while Ethyl acetate AgNPs demonstrated potent α -amylase inhibition. Notably, nanoemulsions of *Z. decumbens* extracts enhanced antihyperglycemic activity but did not significantly improve antimicrobial effects. These findings emphasize the potential of nano-formulations to enhance the therapeutic properties of *Z. decumbens* extracts. Further clinical studies are recommended to explore natural products as safer alternatives to synthetic drugs, offering fewer side effects.

Conflict of interest

There are no conflicts to declare.

Funding sources

This research received no external funding

Acknowledgments

The authors express their appreciation and gratitude to Dr. A. Abd-El-Mogali, a specialized taxonomist at Horticultural Research Institute, Flora & Phyto-taxonomy Research, Agricultural Research Centre, Giza, Egypt, for identifying the plant under investigation.

References

- [1] Petrovic S, Bitá B, Barbinta-Patrascu M-E. Nanoformulations in Pharmaceutical and Biomedical Applications: Green Perspectives. *Int J Mol Sci* 2024, 1:11,5842. <https://doi.org/10.3390/ijms25115842>
- [2] Bakr RO, Tawfike A, El-Gizawy HA, Tawfik N, Abdelmohsen UR, Abdelwahab MF, et al. The metabolomic analysis of five *Mentha* species: cytotoxicity, anti-*Helicobacter* assessment, and the development of polymeric micelles for enhancing the anti-*Helicobacter* activity. *RSC Adv* 2021, 11:13, 7318–30. <https://doi.org/10.1039/D0RA09334C>
- [3] El-Mancy SS, El-Haddad AE, Alshareef WA, Saadeldien AM, El-Emam SZ, Elnahas OS. Enhancement of antimicrobial and antiproliferative activities of standardized frankincense extract using optimized self-nanoemulsifying delivery system. *Sci Pharm* 2021, 89:3, 36. <https://doi.org/https://doi.org/10.3390/scipharm89030036>
- [4] Hamieda S.F. & Saied M. In Vitro Evaluation of Cytotoxicity and Antimicrobial Activity of Green Synthesized Silver Nanoparticles Based on Their Particle Size and Stability. *Egyptian Journal of Chemistry* 2024. <https://doi.org/10.21608/ejchem.2024.328372.10631>
- [5] Al-Abboodi A., Albukhaty S., Sulaiman G. M., Al-Saady M.A.A.J., Jabir M.S. & Abomughaid M.M. Protein Conjugated Superparamagnetic Iron Oxide Nanoparticles for Efficient Vaccine Delivery Systems. *Plasmonics* 2024, 19: 379-388. <https://link.springer.com/article/10.1007/s11468-023-01994-8>
- [6] Neamah S A, Albukhaty S, Falih I Q, Dewir Y H, Mahood H B. Biosynthesis of Zinc Oxide Nanoparticles Using *Capparis spinosa* L. Fruit Extract: Characterization, Biocompatibility, and Antioxidant Activity. *Appl. Sci.* 2023, 13(11), 6604. <https://doi.org/10.3390/app13116604>
- [7] Nosrati H, Heydari M, Khodaei M. Cerium oxide nanoparticles: synthesis methods and applications in wound healing. *Mater Today Bio* 2023, 1:23, 100823. <https://doi.org/10.1016/j.mtbio.2023.100823>
- [8] Ghazy OA, Fouad MT, Morsy TA, Kholif AE. Nanoemulsion formulation of Lawsonia inermis extract and its potential antimicrobial and preservative efficacy against foodborne pathogens. *Food Control* 2023, 145, 109458. <https://doi.org/https://doi.org/10.1016/j.foodcont.2022.109458>
- [9] María Plaza O., Manuel J. S.O., Lozano M.V. Current approaches in lipid-based nanocarriers for oral drug delivery. *Drug Deliv Transl Res.* 2021, 11(2): 471-497. <https://doi.org/10.1007/s13346-021-00908-7>
- [10] Harwansh RK, Deshmukh R, Rahman MA. Nanoemulsion: Promising nanocarrier system for delivery of herbal bioactives. *J Drug Deliv Sci Technol* 2019, 51, 224–33. <https://doi.org/https://doi.org/10.1016/j.jddst.2019.03.006>
- [11] Mady MS, Sobhy Y, Orabi A, Sharaky M, Mina SA, Abo-Zeid Y. Preparation and characterization of nano-emulsion formulations of Asparagus Densiflorus root and aerial parts extracts: Evaluation of in-vitro antibacterial and anticancer activities of nano-emulsion versus pure plant extract. *Drug Dev Ind Pharm* 2024, 50:7, 658–70. <https://doi.org/https://doi.org/10.1080/03639045.2024.2386001>
- [12] Nazeam JA, Ragab GM, El-Gazar AA, El-Mancy SS, Jamil L, Fayez SM. Topical nano clove/thyme gel against genetically identified clinical skin isolates: in vivo targeting behavioral alteration and IGF-1/pFOXO-1/PPAR γ cues. *Molecules* 2021, 26:18, 5608. <https://doi.org/https://doi.org/10.3390/molecules26185608>
- [13] Tominc GC, Dalmagro M, Pereira E da CA, Adamczuk MS, Bonato FGC, Almeida RM de, et al. Formulation and Characterization of Nanoemulsion Incorporating Chamomilla recutita L. Extract Stabilized with Hyaluronic Acid. *Pharmaceutics* 2024, 16:6, 701. <https://doi.org/https://doi.org/10.3390/pharmaceutics16060701>
- [14] Asam Raza M, Farwa U, Waseem Mumtaz M, Kainat J, Sabir A, Al-Sehemi AG. Green synthesis of gold and silver nanoparticles as antidiabetic and anticancerous agents. *Green Chem Lett Rev* 2023, 16:1, 2275666. <https://doi.org/https://doi.org/10.1080/17518253.2023.2275666>
- [15] Barzegar R, Safaei HR, Nemati Z, Ketabchi S, Talebi E. Green synthesis of silver nanoparticles using Zygophyllum qatarense Hadidi leaf extract and evaluation of their antifungal activities. *J Appl Pharm Sci* 2018, 8:03, 168–71. <https://doi.org/10.7324/JAPS.2018.8323>
- [16] Fozia F, Ahmad N, Buoharee ZA, Ahmad I, Aslam M, Wahab A, et al. Characterization and evaluation of antimicrobial potential of Trigonella incise (Linn) mediated biosynthesized silver nanoparticles. *Molecules* 2022, 27:14, 4618. <https://doi.org/10.3390/molecules27144618>
- [17] Rana A, Yadav K, Jagadevan S. A comprehensive review on green synthesis of nature-inspired metal nanoparticles: Mechanism, application and toxicity. *J Clean Prod* 2020, 272:5, 122880. <https://doi.org/10.1016/j.jclepro.2020.122880>
- [18] Restrepo CV, Villa CC. Synthesis of silver nanoparticles, influence of capping agents, and dependence on size and shape: A review. *Environ Nanotechnology, Monit \& Manag.* 2021;15(1):100428. <https://doi.org/10.1016/j.enmm.2021.100428>
- [19] Sun Q, Cai X, Li J, Zheng M, Chen Z, Yu C-P. Green synthesis of silver nanoparticles using tea leaf extract and evaluation of their stability and antibacterial activity. *Colloids surfaces A Physicochem Eng Asp* 2014, 444, 226–31. <https://doi.org/10.1016/j.colsurfa.2013.12.065>
- [20] Prada AL, Keita H, de Souza TP, Lima ES, Acho LDR, da Silva M de JA, et al. Cassia grandis Lf nanodispersion is a hypoglycemic product with a potent α -glucosidase and pancreatic lipase inhibitor effect. *Saudi Pharm J* 2019, 27:2, 191–9. <https://doi.org/https://doi.org/10.1016/j.jsps.2018.10.003>

- [21] Balan K, Qing W, Wang Y, Liu X, Palvannan T, Wang Y, et al. Antidiabetic activity of silver nanoparticles from green synthesis using *Lonicera japonica* leaf extract. *Rsc Adv* 2016, 6:46, 40162–8. <https://doi.org/10.1039/c5ra24391b>
- [22] Meenatchi P, Purushothaman A, Maneemegalai S. Antioxidant, antiglycation and insulinotrophic properties of *Coccinia grandis* (L.) in vitro: Possible role in prevention of diabetic complications. *J Tradit Complement Med* 2017, 7:1, 54–64. <https://doi.org/10.1016/j.jtcme.2016.01.002>
- [23] Shawky E, Gabr N, El-gindi M, Mekky R. A Comprehensive Review on Genus *Zygophyllum*. *J Adv Pharm Res* 2019, 3:1, 1–16. <https://doi.org/10.21608/aprh.2019.5699.1066>
- [24] Clark JL, Zahradka P, Taylor CG. Efficacy of flavonoids in the management of high blood pressure. *Nutr Rev* 2015, 73:12, 799–822. <https://doi.org/10.1093/nutrit/nuv048>
- [25] Hal DM, Eltamany E, Abdelhameed RFA, Ibrahim AK, Badr J, others. Chemical review on *Zygophyllum* genus. *Rec Pharm Biomed Sci* 2022, 6:2, 105–29. <https://doi.org/10.21608/rpbs.2022.148635.1154>
- [26] Syahputra RA, Dalimunthe A, Utari ZD, Halim P, Sukarno MA, Zainalabidin S, et al. Nanotechnology and flavonoids: Current research and future perspectives on cardiovascular health. *J Funct Foods* 2024, 120, 106355. <https://doi.org/https://doi.org/10.1016/j.jff.2024.106355>
- [27] David V, Andrea A-N, Aleksandr K, Lourdes J-A, Eugenia P, Nancy C, et al. Validation of a method of broth microdilution for the determination of antibacterial activity of essential oils. *BMC Res Notes* 2021, 14:1, 439. <https://doi.org/10.1186/s13104-021-05838-8>
- [28] Esawy MA, Ragab TIM, Basha M, Emam M, others. Evaluated bioactive component extracted from *Punica granatum* peel and its Ag NPs forms as mouthwash against dental plaque. *Biocatal Agric Biotechnol* 2019, 18, 101073. <https://doi.org/https://doi.org/10.1016/j.bcab.2019.101073>
- [29] Zayed MF, Eisa WH, Shabaka AA. *Malva parviflora* extract assisted green synthesis of silver nanoparticles. *Spectrochim Acta Part A Mol Biomol Spectrosc* 2012, 98, 423–8. <https://doi.org/10.1016/j.saa.2012.08.072>
- [30] Antunes Filho S, Backx BP. Nanotecnologia e seus impactos na sociedade. *Rev Tecnol e Soc* 2020, 16:40, 1–15. 10.3895/rt.s.v16n40.9870.
- [31] Fiori JL, Shin Y-K, Kim W, Krzysik-Walker SM, González-Mariscal I, Carlson OD, et al. Resveratrol prevents β -cell dedifferentiation in nonhuman primates given a high-fat/high-sugar diet. *Diabetes* 2013, 62:10, 3500–13. <https://doi.org/10.2337/db13-0266>
- [32] Shahidi F, Danielski R. Review on the Role of Polyphenols in Preventing and Treating Type 2 Diabetes: Evidence from In Vitro and In Vivo Studies. *Nutrients* 2024, 16:18, 3159. <https://doi.org/https://doi.org/10.3390/nu16183159>
- [33] Lunagariya NA, Patel NK, Jagtap SC, Bhutani KK. Inhibitors of pancreatic lipase: state of the art and clinical perspectives. *EXCLI J* 2014, 13, 897. <https://pubmed.ncbi.nlm.nih.gov/26417311/>
- [34] Khare A, Ansari A, Patki P, Perampalli N. Design and Development of Nanoemulsions Formulation: a Review. *Int J Creat Res Thoughts* 2021, 9:7, 2320–2882 <https://ijcrt.org/papers/IJCRT2107133.pdf>
- [35] Hamid KM, Wais M, Sawant G. A review on nanoemulsions: formulation, composition, and applications. *Asian J Pharm Clin Res* 2021, 14:4, 22–28. <https://doi.org/10.22159/ajpcr.2021.v14i4.40859>
- [36] Chung I-M, Park I, Seung-Hyun K, Thiruvengadam M, Rajakumar G. Plant-mediated synthesis of silver nanoparticles: their characteristic properties and therapeutic applications. *Nanoscale Res Lett* 2016, 11, 1–14. <https://doi.org/10.1186/s11671-016-1257-4>
- [37] Ghazy OA, Fouad MT, Saleh HH, Kholif AE, Morsy TA. Ultrasound-assisted preparation of anise extract nanoemulsion and its bioactivity against different pathogenic bacteria. *Food Chem* 2021, 341:2, 128259. <https://doi.org/10.1016/j.foodchem.2020.128259>
- [38] Emam M, El Raey MA, Eisa WH, El-Haddad AE, Osman SM, El-Ansari MA, et al. Green synthesis of silver nanoparticles from *Caesalpinia gilliesii* (Hook) leaves: antimicrobial activity and in vitro cytotoxic effect against BJ-1 and MCF-7 cells. *J Appl Pharm Sci* 2017, 7:8, 226–33. <https://doi.org/10.7324/JAPS.2017.70831>
- [39] Hasanin MS, Emam M, Soliman MMH, Latif RRA, Salem MMM, El Raey MA, et al. Green silver nanoparticles based on *Lavandula coronopifolia* aerial parts extract against mycotic mastitis in cattle. *Biocatal Agric Biotechnol* 2022, 42, 102350. <https://doi.org/https://doi.org/10.1016/j.bcab.2022.102350>
- [40] El-Mancy SS, Boshra SA, Elnahas OS, Fayeze SM, Sheta NM. Enhancement of Bottle Gourd Oil Activity via Optimized Self-Dispersing Lipid Formulations (SDLFs) to Mitigate Isoproterenol-Evoked Cardiac Toxicity in Rats via Modulating BNP, MMP2, and miRNA-21 and miRNA-23a Genes' Expression. *Molecules* 2023, 28:16, 6168. <https://doi.org/https://doi.org/10.3390/molecules28166168>
- [41] Abdallah HM, Kashegari AT, Shalabi AA, Darwish KM, El-Halawany AM, Algandaby MM, et al. Phenolics from *Chrozophora oblongifolia* aerial parts as inhibitors of α -glucosidases and advanced glycation end products: in-vitro assessment, molecular docking and dynamics studies. *Biology (Basel)* 2022, 11:5,762. <https://doi.org/10.3390/biology11050762>
- [42] Khadayat K, Marasini BP, Gautam H, Ghaju S, Parajuli N. Evaluation of the alpha-amylase inhibitory activity of Nepalese medicinal plants used in the treatment of diabetes mellitus. *Clin Phytoscience* 2020, 6:34, 1–8. <https://doi.org/10.1186/s40816-020-00179-8>